HHS Public Access

Author manuscript

Cancer Lett. Author manuscript; available in PMC 2024 April 10.

Published in final edited form as:

Cancer Lett. 2023 April 10; 559: 216116. doi:10.1016/j.canlet.2023.216116.

MUC1-C IS NECESSARY FOR SHP2 ACTIVATION AND BRAF INHIBITOR RESISTANCE IN BRAF(V600E) MUTANT COLORECTAL CANCER

Yoshihiro Morimoto[1], **Nami Yamashita**[1], **Haruka Hirose**[2], **Atsushi Fushimi**[1], **Naoki Haratake**[1], **Tatsuaki Daimon**[1], **Atrayee Bhattacharya**[1], **Rehan Ahmad**[1], **Yozo Suzuki**[3], **Hidekazu Takahashi**[3], **Donald W. Kufe**[1,*]

[1]Dana-Farber Cancer Institute, Harvard Medical School, Boston, MA

[2]Division of Systems Biology, Nagoya University Graduate School of Medicine, Nagoya 466-8550, Japan

[3]Department of Gastroenterological Surgery, Graduate School of Medicine, Osaka University, Suita, Osaka 565-0871, Japan

Abstract

Colorectal cancers (CRCs) harboring the BRAF(V600E) mutation are associated with aggressive disease and resistance to BRAF inhibitors by feedback activation of the receptor tyrosine kinase (RTK)→RAS→MAPK pathway. The oncogenic MUC1-C protein promotes progression of colitis to CRC; whereas there is no known involvement of MUC1-C in BRAF(V600E) CRCs. The present work demonstrates that MUC1 expression is significantly upregulated in BRAF(V600E) vs wild-type CRCs. We show that BRAF(V600E) CRC cells are dependent on MUC1-C for proliferation and BRAF inhibitor (BRAFi) resistance. Mechanistically, MUC1-C integrates induction of MYC in driving cell cycle progression with activation of the SHP2 phosphotyrosine phosphatase, which enhances RTK-mediated RAS→ERK signaling. We demonstrate that targeting MUC1-C genetically and pharmacologically suppresses (i) activation of MYC, (ii) induction of the NOTCH1 stemness factor, and (iii) the capacity for self-renewal. We also show that MUC1-C associates with SHP2 and is required for SHP2 activation in driving BRAFi-induced feedback of ERK signaling. In this way, targeting MUC1-C in BRAFi-resistant BRAF(V600E) CRC tumors inhibits growth and sensitizes to BRAF inhibition. These findings demonstrate that MUC1-C is a target for the treatment of BRAF(V600E) CRCs and for reversing their resistance to BRAF inhibitors by suppressing the feedback MAPK pathway.

[*]**Corresponding author:** Donald Kufe, 450 Brookline Avenue, D830, Boston, Massachusetts, 02215 donald_kufe@dfci.harvard.edu.

Authors Contribution

Conceptualization: Y.M. and D.W.K.; Methodology: Y.M. and D.W.K.; Validation: Y.M., N.Y., H.H., A.F., N.H., T.D., A.B., R.A., Y.S., and H.T.; Investigation: Y.M., N.Y., H.H., A.F., N.H., T.D., A.B., R.A., Y.S., and H.T.; Resources: Y.M., H.H., A.F., and Y.S.; Data curation: Y.M., H.H., and A.F.; Writing – original draft: Y.M. and D.W.K.; Writing – review & editing: Y.M. and D.W.K.; Visualization: Y.M., N.Y., H.H., and A.F.; Supervision: D.W.K; Project Administration: Y.M., N.Y. and D.W.K; and Funding acquisition: D.W.K.

Conflict of interest statement: DK has equity interests in Genus Oncology, Reata Pharmaceuticals and HillstreamBiopharma and is a paid consultant to Reata and CanBas. The other authors declared no potential conflicts of interest.

Keywords

MUC1-C; CRC; BRAF(V600E); SHP2; BRAF inhibitor resistance

1. Introduction

BRAF mutations occur in 8–12% of CRCs and are mutually exclusive with alterations in the *KRAS* gene (1, 2). Approximately 90% of *BRAF* mutations involve substitution of valine by glutamine in codon 600 (V600E)(1). Patients with CRCs that are *BRAF* mutant have a median overall survival (OS) of 10.4 months as compared to 34.7 months for those with *BRAF* wild-type (WT) tumors (1–3). *BRAF* mutant CRCs are often associated with a CpG island methylator phenotype (CIMP) and high microsatellite instability (MSI-H)(1–3). As compared to *BRAF* WT CRCs, *BRAF* mutant tumors also have a unique clinical presentation in the right-sided proximal colon that is more prevalent in women and patients over 65 years of age (1, 2, 4). In addition, CRCs harboring *BRAF* mutations are often poorly differentiated with a mucinous histology that, unlike wild-type tumors, spread to the peritoneum and distant lymph nodes (1, 5). Another distinguishing characteristic of *BRAF* mutant CRCs is therapeutic resistance. In contrast to melanomas with *BRAF* mutations that are highly sensitive to BRAF kinase inhibitors, such as vemurafenib, dabrafenib and encorafinib, only 5% of BRAF(V600E) CRCs respond to these agents (1, 2). This distinction in response rates has been attributed to the marked suppression of downstream MAPK signaling in BRAF(V600E) melanomas and only transient inhibition of this pathway in BRAF(V600E) CRCs, which is associated with feedback activation of receptor tyrosine kinases (RTKs) (6–8). Accordingly, dabrafenib has been combined with the MEK inhibitor trametinib to achieve sustained MAPK suppression in BRAF(V600E) CRC cell lines (9); although this combination has had limited activity in patients with BRAF(V600E) CRC (2, 3, 10). Combined targeting of (i) BRAF(V600E), EGFR and MEK, or (ii) BRAF(V600E), EGFR and PI3K has also had limited clinical benefit in the treatment of BRAF(V600E) CRCs (1–3, 11), underscoring the need for identifying other therapeutic targets for these recalcitrant malignancies.

The *MUC1* gene encodes a non-covalent heterodimeric complex that evolved in mammals to protect barrier tissues from loss of homeostasis (12–14). The MUC1 N-terminal (MUC1-N) and C-terminal (MUC1-C) subunits are expressed at the apical borders of epithelia lining the gastrointestinal tract and other organs (13, 14). In response to infections and damage, MUC1-N is shed into a protective mucous gel and MUC1-C is activated to transduce inflammatory, proliferative and remodeling signals associated with wound repair (13–15). Prolonged activation of MUC1-C, for example in response to chronic inflammation, promotes carcinogenesis and the cancer stem cell (CSC) state (13–15). In this way, MUC1-C induces the Yamanaka OCT4, SOX2, KLF4 and MYC (OSKM) pluripotency factors, which are repressed in somatic cells, but are reactivated in wound healing and cancer (13–15). MUC1-C also induces the epithelial-mesenchymal transition (EMT) and epigenetic reprogramming by activation of the Polycomb Repressive Complexes 1 (PRC1) and PRC2 (16). Embryonic stem cells are driven by the reorganization of chromatin at enhancers during reprogramming (17), in part, by the recruitment of SWI/SNF chromatin remodeling

complexes (18–20). Along these lines, MUC1-C activates the embryonic stem BAF (esBAF) and poly-bromo PBAF complexes in CSCs (21, 22) and induces chromatin remodeling at enhancer-like signatures in stemness-associated genes, such as *NOTCH1* (23). Studies in a colitis model of chronic inflammation demonstrated induction of MUC1-C and the CSC state in progression to CRC (24). In addition, targeting MUC1-C suppressed stemness and the progression of colitis to colon carcinoma, supporting involvement of MUC1-C in resident SC lineage plasticity in this setting of chronic inflammation (24). However, it is not known if MUC1-C drives BRAF(V600E) CRC progression and resistance to treatment, which remains an unmet therapeutic challenge.

A recent meta-analysis of CRC studies found that MUC1 significantly associates with advanced tumor stage and poor overall survival (25); however, this work did not include investigation of BRAF mutation status. Whereas *BRAF* mutant CRCs often exhibit the MSI-H genotype (1–3), other work has demonstrated that MUC1 has no significant association with MSI status in CRC (26). Thus, to our knowledge, there is no available evidence linking MUC1 to BRAF(V600E) mutant CRC. The present studies demonstrate that MUC1 is upregulated in BRAF(V600E) mutant vs wild-type CRC tumors. We show that MUC1-C-induced activation of MYC is necessary for cell cycle progression and the CSC state of BRAF(V600E) CRC cells. There is no known involvement of MUC1-C in regulation of the SHP2 phosphotyrosine phosphatase. Importantly, we report that MUC1-C is required for SHP2 activation and feedback induction of ERK in response to BRAF inhibitors. In concert with these results, we demonstrate that MUC1-C is necessary for (i) self-renewal and tumorigenicity of BRAF(V600E) CRC cells, and (ii) intrinsic and acquired resistance of BRAF(V600E) CRC cells to BRAF inhibition. These findings identify MUC1-C as a target for the treatment of aggressive and drug-resistant BRAF(V600E) CRCs.

2. Materials and Methods

Analysis of human CRC tumors.

Data from the Cancer Genome Atlas (TCGA) COAD cohortthat included overall survival (OS) and corresponding RNA-seq expression (FPKM values) were downloaded from TCGAbiolinks(version 2.22.1) using GDCquery. Values were converted to TPM (transcripts per kilobase million) for subsequent analysis. Mutation data were analyzed using maftools(version 2.10.5). Survival analysis was performed using the survival package(version 3.4.0) in R. Cox regression was used to estimate the difference in survival between patients with NOTCH1-high and NOTCH1-low gene expression. Available information on the patient's last follow-up or time of death was used for analysis. Kaplan-Meier curves were drawn using the R library survminer(version 0.4.9).

Cell culture.

RKO BRAF(V600E) cells (ATCC, Manassas, VA, USA) were cultured in EMEM medium (Thermo Fisher Scientific, Waltham, MA, USA) supplemented with 10% fetal bovine serum (FBS; GEMINI Bio-Products, West Sacramento, CA, USA). LS411N BRAF(V600E) cells (ATCC) were cultured in RPMI1640 medium supplemented with 10% FBS. Cells were treated with the MUC1-C inhibitor GO-203 (13–15). Authentication of the cells was

performed by short tandem repeat (STR) analysis. Cells were monitored for mycoplasma contamination using the MycoAlert Mycoplasma Detection Kit (Lonza, Rockland, MA, USA). Cells were maintained for 3 months when performing experiments.

Gene silencing.

MUC1shRNA (MISSION shRNA TRCN0000122938; Sigma, St. Louis, MO, USA), MYCshRNA (MISSION shRNA TRCN0000039642; Sigma) or a control scrambled shRNA (CshRNA; Sigma) was inserted into the pLKO-tet-puro vector (Plasmid #21915; Addgene, Cambridge, MA, USA) as described (27). The MUC1shRNA#2 (MISSION shRNA TRCN0000430218) was produced in HEK293T cells as described (28). Cells transduced with the vectors were selected for growth in 1–2 μg/ml puromycin. Cells were treated with 0.1% DMSO as the vehicle control or 500 ng/ml DOX (Millipore Sigma).

Quantitative reverse-transcription PCR (qRT-PCR).

Total cellular RNA was isolated using Trizol reagent (Thermo Fisher Scientific). cDNAs were synthesized using the High Capacity cDNA Reverse Transcription Kit (Applied Biosystems, Grand Island, NY, USA) as described (27). The cDNA samples were amplified using the Power SYBR Green PCR Master Mix (Applied Biosystems) and the CFX96 Real-Time PCR System (BIO-RAD, Hercules, CA, USA) as described (27). Primers used for qRT-PCR are listed in Supplementary Table S1.

Immunoblot analysis.

Total lysates prepared from non-confluent cells were subjected to immunoblot analysis using anti-MUC1-C (HM-1630-P1ABX, 1:1000 dilution; Thermo Fisher Scientific), anti-β-actin (A5441, 1:5000 dilution; Sigma-Aldrich), anti-MYC (ab32072, 1:1000 dilution; Abcam, Waltham, MA, USA), anti-CDK4 (12790, 1:1000 dilution; Cell Signaling Technology (CST), Danvers, MA, USA), anti-CDK6 (3136, 1:1000 dilution; CST), anti-p-RB (9307, 1:1000 dilution; CST), anti-RB (9309, 1:1000 dilution; CST), anti-cyclin A2 (4656, 1:1000 dilution; CST), Danvers, MA, USA), anti-cyclin B1 (4138, 1:1000 dilution; CST), anti-SHP2 (3752, 1:1000 dilution; CST), anti-p-SHP2 (3751, 1:1000 dilution; CST), anti-BRG1 (ab110641,1:10000 dilution; CST), anti-ARID1A (12354, 1:1000 dilution; CST), anti-BAF155 (11956, 1:5000 dilution; CST), anti-NOTCH1 (3608, 1:1000 dilution; CST), anti-HES1 (11988, 1:1000 dilution; CST), anti-MEK (8727, 1:1000 dilution; CST), anti-EGFR (2232, 1:1000 dilution); CST, anti-p-EGFR (2234, 1:1000 dilution; CST), anti-p-MEK (9121, 1:1000 dilution; CST), anti-ERK (4695, 1:1000 dilution; CST), anti-p-ERK (4377, 1:1000 dilution; CST), anti-AKT (9272, 1:1000 dilution; CST) and anti-p-AKT (4058, 1:1000 dilution; CST).

RNA-seq analysis.

Total RNA from cells cultured in triplicates was isolated using the RNeasy Plus Mini Kit (Qiagen). TruSeq Stranded mRNA (Illumina, San Diego, CA, USA) was used for library preparation as described (29). Raw sequencing reads were aligned to the human genome (GRCh38.74) with STAR as described (29). Raw feature counts were normalized and differential expression analysis was performed using DESeq2 as described (29). The fgsea

(v1.8.0) package in R was used for differential expression rank order and GSEA. Gene sets queried included those available through the Molecular Signatures Database (MSigDB) as described (29).

Coimmunoprecipitation studies.

Protein lysates were immunoprecipitated with anti-SHP2 (3397, CST) or a rabbit isotype control IgG (3900S, CST) using the Pierce Classic Magnetic Co-IP Kit (Thermo Fisher Scientific).

Colony formation assays.

Cells were seeded in 24-well plates for 24 hours and then (i) treated with vehicle or 500 ng/ml DOX, or (ii) left untreated or treated with GO-203. After 7–10 days, cells were stained with 0.5% crystal violet (LabChem, Zelienople, PA, USA) in 25% methanol. Colonies >25 cells were counted in triplicate wells.

Tumorsphere formation assays.

Cells ($2–6 \times 10^3$) were seeded per well in 6-well ultra-low attachment culture plates (Corning Life Sciences) in DMEM/F12 50/50 medium (Corning Life Sciences) with 20 ng/ml EGF (Millipore Sigma), 20 ng/ml bFGF (Millipore Sigma) and 1% B27 supplement (Gibco). In certain studies, cells were treated with (i) 500 ng/ml DOX, (ii) GO-203, (iii) PLX4720 (Selleck Chemicals, Houston, TX, USA) or (iv) SHP099 (Selleck Chemicals, Houston, TX, USA). Tumorspheres were counted under an inverted microscope in triplicate wells.

Isobologram analysis.

Cells ($3–5\times10^3$) were seeded per well in 96 well plates (Thermo Fisher Scientific) and incubated for 24 hours. The cells were then left untreated or treated with 0.25 to 2 μM GO-203 in the presence of varying concentrations of PLX4720 for 92 hours. Cell viability was assessed by Alamar Blue staining and used to calculate the IC50 values of PLX4720 at each concentration of GO-203. Values under the additive line were denoted as synergistic.

Mouse tumor xenograft studies.

Six- to 8-week old nude mice (Taconic Farms, Germantown, NY, USA) were injected subcutaneously in the flank with $1–3 \times 10^6$ RKO or LS411N-BR cells in 100 μl of a 1:1 solution of medium and Matrigel (BD Biosciences). When the mean tumor volume reached 100–150 mm^3, mice were pair-matched into groups of 6 mice each. Mice were treated intraperitoneally each day for 19 days with PBS or GO-203 at a dose of 12 μg/gm body weight in the absence and presence of oral PLX4720 administration. Irradiated PLX4720 diet was purchased from Research Diets (New Brunswick, NJ, USA) and dosed at a concentration of 417 mg/kg/day. Unblinded tumor measurements and body weights were recorded twice each week. Mice were sacrificed on day 19 when control tumors reached >2000 mm^3 as calculated by the formula: $(width)^2$ x length/2. The resource equation method was used to determine the minimum number of mice for achieving significance (30).

Study Approval.

The *in vivo* studies were conducted in accordance with ethical regulations required for approval by the Dana-Farber Cancer Institute Animal Care and Use Committee (IACUC) under protocol 03–029.

Statistics.

Each experiment was performed at least three times. Data are expressed as the mean±SD. The unpaired Mann-Whitney U test was used to determine differences between means of groups. A pvalue of <0.05 denoted by an asterisk (*) was considered statistically significant.

Data and materials availability:

The accession numbers for the RNA-seq data are GEO Submission GSE215849 and GSE215308.

3. Results

MUC1-C regulates cell cycle progression in BRAF(V600E) mutant CRC cells.

Analysis of the TCGA_COAD dataset demonstrated that MUC1 is significantly upregulated in BRAF(V600E) mutant, as compared to wild-type BRAF, CRCs (Fig. 1A). To investigate the potential significance of this finding, we established human RKO BRAF(V600E) mutant cells expressing a tet-inducible control shRNA (tet-CshRNA) or a tet-MUC1shRNA. Treatment with doxycycline (DOX) downregulated MUC1-C expression in RKO/tet-MUC1shRNA, but not tet-CshRNA, cells (Fig. 1B). RNA-seq analysis of RKO/tet-MUC1shRNA cells without and with MUC1-C silencing demonstrated that MUC1-C activates 3301 and represses 3458 genes (Fig. 1C). GSEA further demonstrated that silencing MUC1 associates with significant suppression of the BENPORATH_PROLIFERATION (Fig. 1D), BENPORATH_CYCLING_GENES (Fig. 1E), REACTOME_CELL CYCLE_MITOTIC (Fig. 1F) and GO_MITOTIC_CELL_CYCLE (Supplemental Fig. S1A) gene signatures, indicating that MUC1-C is necessary for RKO cell cycle progression. Along these lines, silencing MUC1-C in RKO cells was associated with inhibition of proliferation (Supplemental Fig. S1B).

RKO BRAF(V600E) mutant cells also harbor a PIK3CA mutation, which activates the AKT pathway and confers intrinsic resistance to BRAFis (31). In contrast, LS411N BRAF(V600E) mutant cells, which express wild-type PIK3CA, exhibit upregulation of EGFR activation in response to loss of the ERK-mediated negative feedback pathway (32). Along these lines, treatment of RKO cells with the BRAFi PLX4720 demonstrated an IC50=11.6 μM, whereas LS411N BRAF(V600E) CRC cells are more sensitive to PLX472O with an IC50=2.09 μM (Fig. 2A). To establish a model of adaptive resistance, LS411N cells were exposed to increasing concentrations of PLX4720 and thereby the selection of BRAFi-resistant LS411N-BR cells (IC50=29.0 μM) (Fig. 2A). Analysis of RKO, LS411N and LS411N-BR cells demonstrated that LS411N-BR cells exhibit upregulation of (i) p-EGFR compared to RKO and LS411N cells and (ii) p-MEK and p-ERK vs LS411N cells (Supplemental Fig. S2A). LS411N and LS411N-BR cells were then transfected to express the tet-MUC1shRNA vector to assess the

effects of silencing MUC1 on their transcriptomes (Supplemental Figs. S2B and S2C). RNA-seq analysis demonstrated that suppression of MUC1-C expression in LS411N (Supplemental Fig. S2D) and LS411N-BR (Supplemental Fig. S2E) cells is associated with overlapping down- and up-regulated gene sets (Fig. 2B). In addition and as found in RKO cells, silencing MUC1 in LS411N and LS411N-BR cells was associated with significant suppression of the BENPORATH_PROLIFERATION (Supplemental Fig. S2F), BENPORATH_CYCLING_GENES (Fig. 2C) and REACTOME_CELL CYCLE_MITOTIC (Fig. 2D) gene signatures. Consistent with these results, analysis of downregulated genes in the BENPORATH _CYCLING_GENES signature demonstrated overlap with MUC1 silencing in RKO, LS411N and LS411N-BR cells (Fig. 2E). Among these genes, we identified *CDK6,* which encodes cyclin-dependent kinase 6 (CDK6), an effector of RB phosphorylation, release of E2F and cell entry into S phase (33). We also identified *CCNA2* and *CCNB1,* which encode the cyclin A2 and cyclin B1 proteins, respectively, that activate CDK1, a master regulator of cell cycle progression and gene transcription (34, 35). We found that silencing MUC1-C in RKO cells has little effect on CDK4, but results in downregulation of the CDK6, p-RB, cyclin A2 and cyclin B1 proteins (Fig. 2F). We also found that expression of CDK6, p-RB, cyclin A2 and cyclin B1 is upregulated in LS411N-BR vs LS411 cells (Fig. 2G) by a MUC1-C-dependent mechanism (Fig. 2H). Moreover and as found in RKO cells, silencing MUC1-C inhibited LS411N and LS411N-BR cell growth (Supplemental Fig. S2G).

MUC1-C regulates activation of MYC and SHP2 signaling in BRAF(V600E) CRC cells.

The MUC1-C cytoplasmic domain (CD) is phosphorylated by multiple RTKs and interacts with effectors, such as PI3K, SHC, PLCgamma and GRB2, that contribute to RTK→RAS signaling (Fig. 3A) (14). MUC1-C/CD also binds directly to MYC and regulates the expression of MYC target genes (Fig. 3A) (13–15, 36). Consistent with this function, silencing MUC1-C in RKO and LS411N-BR cells was associated with significant repression of the HALLMARK MYC TARGETS V1 gene signature (Fig. 3B). We confirmed that silencing MYC in RKO and LS411N-BR cells decreases CDK6, cyclin A2 and cyclin B1 expression, supporting involvement of the MUC1-C→MYC pathway in driving cell cycle progression (Fig. 3C). Adjacent to the MYC binding site in MUC1-C/CD is a sequence (YGQLD) (Fig. 3A) that, when phosphorylated (pYGQLD), is shared with (i) pYLALD in GAB2 (p97), (ii) pYGELD in PD-1, and (iii) pYIDLD in IRS1 for binding of the SHP2 phosphotyrosine phosphatase N-terminal SH2 domain (37–39). Coimmunoprecipitation studies demonstrated that MUC1-C associates with SHP2 in RKO and LS411N-BR cells (Fig. 3D). In addition and importantly, silencing MUC1-C in RKO and LS411N-BR cells suppressed SHP2 activation as evidenced by decreases in p-SHP2(Y542) (Fig. 3E; Supplemental Fig. S3A). The MUC1-C inhibitor GO-203 blocks the MUC1-C CQC motif that binds to MYC, inhibits MUC1-C dimerization and phenocopies the effects of MUC1-C silencing (13–15). Treatment of RKO and LS411N-BR cells with GO-203 inhibited the interaction between MUC1-C and SHP2 (Fig. 3F; Supplemental Fig. S3B) and suppressed p-SHP2(Y542) levels (Fig. 3G), confirming that MUC1-C is necessary for SHP2 activation. Notably, silencing MYC in RKO and LS411N-BR cells had no apparent effect on SHP2 activation (Supplemental Fig. S3C). Moreover, treatment of RKO and LS411N-BR cells with the SHP2 inhibitor SHP099 had little if any effect on MYC, CDK6, cyclin A2 and

cyclin B1 expression (Supplemental Fig. S3D), in support of a model in which MUC1-C independently regulates (i) SHP2 activation, and (ii) the MYC→CDK6/cyclin A2/cyclin B1 pathway.

MUC1-C activates esBAF and stemness-associated genes in BRAF(V600E) CRC cells.

CDK6-mediated RB phosphorylation promotes cell cycle entry and releases E2F in driving gene transcription (33). Consistent with the effects of MUC1-C on CDK6 and p-RB, we found that silencing MUC1-C in RKO and LS411N-BR cells suppresses the HALLMARK E2F TARGET GENE signature (Fig. 4A). MUC1-C→E2F1 signaling activates the SWI/SNF esBAF chromatin remodeling complex (14, 21–23). Here, we found that silencing MUC1-C in BRAF(V600E) cells significantly suppresses (i) the GOCC_SWI_SNF_COMPLEX and GOCC_SWI_SNF_SUPERFAMILY_TYPE_COMPLEX gene signatures (Supplemental Figs. S4A and S4B) and (ii) expression of the BRG1, ARID1A and BAF155 components of the esBAF complex (Fig. 4B). The MUC1-C→esBAF pathway increases chromatin accessibility of stemness-associated genes in driving the CSC state (23). In support of those findings, silencing MUC1-C in RKO and LS411N-BR cells was significantly associated with downregulation of the BENPORATH_ES_1 signature derived from genes enriched in ESCs and poorly differentiated cancers (Fig. 4C) (40). Overlap of the downregulated genes in RKO and LS411N-BR cells identified 1773, which included *NOTCH1,* an important effector in driving the CSC state (23) (Fig. 4D). We confirmed that MUC1-C is necessary for expression of NOTCH1 and the downstream HES1 effector of stemness (Fig. 4E). Moreover, MUC1 expression in RKO and LS411N-BR cells was significantly associated with activation of the REACTOME_SIGNALING_BY_NOTCH gene signature (Fig. 4F). Of further interest, we found that MYC (Fig. 4G), but not SHP2 (Supplemental Fig. S4C), is necessary for NOTCH1 expression, indicating that the MUC1-C→MYC pathway, and not MUC1-C→SHP2 activation, drives stemness in BRAFi-resistant BRAF(V600E) CRC cells.

MUC1-C is necessary for feedback activation of p-ERK in response BRAFi treatment.

BRAFi treatment of BRAF(V600E) CRC cells is associated with feedback activation of the RTK→RAS→MAPK pathway and drug resistance. To determine if MUC1-C-induced activation of MYC and/or SHP2 plays a role in conferring BRAFi resistance, we first assessed the effects of silencing MUC1-C on sensitivity to PLX4720, a preclinical analog of vemurafenib that selectively targets BRAF(V600E). Silencing MUC1-C in RKO/tet-MUC1shRNA cells treated with DOX significantly suppressed RKO colony formation and also enhanced the anti-proliferative effects of PLX4720 (Fig. 5A). Analysis of LS411N-BR/tet-MUC1shRNA cells further demonstrated that silencing MUC1-C completely inhibits colony formation (Fig. 5B). These effects were associated with suppression of p-SHP2, p-MEK, p-ERK and p-AKT activation (Figs. 5C and 5D), consistent with downregulation of RTK→RAS→MAPK signaling. In addition and based on involvement of MUC1-C in the MYC pathway, we found downregulation of CDK6, cyclin A2 and cyclin B1 (Supplemental Figs. S5A and S5B). By extension, treatment with GO-203 also suppressed colony formation and increased sensitivity to PLX4720 in RKO (Fig. 5E) and LS411N-BR (Fig. 5F) cells. In addition, combining GO-203 and PLX4720 (i) suppressed CDK6, cyclin A2 and cyclin B1 expression (Supplemental Figs. S5C and S5D), and (ii) downregulated

p-SHP2, p-MEK, p-ERK and p-AKT levels (Figs. 5G and 5H), indicating that MUC1-C is necessary for cell cycle progression and activation of the BRAFi-induced MAPK feedback pathway.

MUC1-C is required for self-renewal capacity of BRAF(V600E) CRC cells.

To extend these studies to effects of targeting MUC1-C and BRAF(V600E) on self-renewal capacity, we analyzed RKO/tet-MUC1shRNA cells growing as tumorspheres in 3D culture. Silencing MUC1-C was associated with a significant decrease in tumorsphere formation and potentiation of PLX4720 treatment (Fig. 6A). In concert with involvement of the MUC1-C→MYC→NOTCH1 pathway in self-renewal, we also found downregulation of ERK-mediated p-MYC(Ser62) activation and NOTCH1 expression (Fig. 6B). Similar results were obtained in studies of LS411N-BR/tet-MUC1shRNA cells (Figs. 6C and 6D). We confirmed that these effects of targeting MUC1-C are conferred by MYC as evidenced by the demonstration that silencing MYC suppresses (i) self-renewal capacity (Figs. 6E and 6F), and (ii) NOTCH1 expression (Figs. 6G and 6H). Of further interest, treatment of RKO and LS411N-BR cells with SHP099 and PLX4720 inhibited self-renewal and NOTCH1 (Supplemental Figs. S6A–S6D), indicating that MUC1-C integrates activation of MYC and SHP2 in the setting of BRAF(V600E) inhibition.

MUC1-C is necessary for BRAFi resistance in BRAF(V600E) CRC cells.

Dedifferentiation and lineage plasticity endows cancer cells with the capacity for drug resistance (41–44). The findings that MUC1-C is necessary for self-renewal of BRAF(V600E) CRC cells invoked the possibility that MUC1-C signaling through MYC or SHP2 also contributes to BRAFi resistance. Along these lines, isobologram analyses of RKO and LS411N-BR cells treated with different GO-203 and PLX4720 concentrations demonstrated synergistic activity (Figs. 7A and 7B). GO-203 treatment of RKO and LS411N-BR cells also potentiated the effects of PLX4720 on suppression of (i) tumorsphere formation (Figs. 7C and 7D), and (ii) p-MEK, p-ERK, p-MYC(Ser-62) and NOTCH1 expression (Figs. 7E and 7F). In concert with these results, treatment of RKO and LS411N-BR tumors with PLX4720 alone had little if any effect (Figs. 7G and 7H). By contrast, GO-203 as a single agent, which was administered daily because of a short circulating half-life (45), inhibited tumor growth and the combination of GO-203 and PLX4720 was more effective than either agent used alone (Figs. 7G and 7H). Moreover, combining GO-203 and PLX4720 was well tolerated as supported by the absence of significant weight loss (Supplemental Figs. S7A and S7B).

Induction of NOTCH1 in BRAF(V600E) vs BRAF WT CRCs is associated with poor clinical outcomes.

Patients with *BRAF* mutant CRCs have a median OS of 10.4 months vs 34.7 months for those with *BRAF* WT tumors (1–3). The basis for this difference is not known; however, the CSC state is associated with lineage plasticity, DNA damage resistance, immune evasion and poor clinical outcomes (41–44). Our findings that the MUC1-C→MYC→NOTCH1 pathway promotes self-renewal invoked the possibility that activation of NOTCH1 contributes to decreases in survival in patients with BRAF(V600E) CRCs. In support of this notion, we found that NOTCH1 expression in BRAF(V600E) CRCs is associated with

a significant decrease in survival (Fig. 8A). In contrast, there was no significant association of NOTCH1 expression with survival of patients with BRAF WT CRCs (Fig. 8B), supporting the potential clinical importance of the MUC1-C→MYC→NOTCH1 pathway in contributing to aggressiveness of BRAF(V600E) CRCs.

4. Discussion

Patients with CRCs harboring the BRAF(V600E) mutation have a substantially decreased median OS compared to those with wild-type *BRAF* tumors (1–3). BRAF(V600E) CRCs are also associated with BRAFi resistance resulting from feedback activation of the EGFR→MAPK pathway (6, 7). Attempts at targeting BRAF(600E), EGFR and MEK have had limited clinical activity in the treatment of BRAF(V600E) CRCs (1–3), in support of alternative mechanisms responsible for the associated poor survival and BRAFi resistance. The present work has identified upregulation of MUC1 expression in BRAF(V600E) CRCs, as compared to those with WT BRAF. MUC1-C is activated by chronic inflammation and promotes the progression of colitis to CRC (13, 24, 46). However, whether MUC1-C contributes to aggressiveness or drug resistance of certain CRCs has remained an unexplored issue. Accordingly, we studied RKO BRAF(V600E) cells and found that MUC1-C is necessary for the expression of cell cycle gene signatures. Similar results were obtained in LS411N BRAF(600E) cells, which were confirmed in both cell types with dependency on MUC1-C for proliferation. MUC1-C induces MYC expression and, in addition, binds to the MYC HLH-LZ domain (36, 47). In this way, MUC1-C regulates the expression of MYC target genes, that include *CDK6, CCNA2* and *CCNB1* (48). CDK6 phosphorylates p-RB, releases E2F and promotes entry into the cell cycle (33). Cyclin A2 and cyclin B1 activate CDK1, which also promotes cell cycle progression and gene transcription (34, 35). We found that silencing MUC1-C and MYC in RKO and LS411N cells suppresses CDK6, p-RB, cyclin A2 and cyclin B1 expression, supporting the importance of the MUC1-C→MYC pathway for proliferation of BRAF(V600E) mutant CRC cells (Fig. 8C).

BRAF(V600E) CRCs are largely unresponsive to vemurafenib, dabrafenib and encorafinib (1, 2). We confirmed that RKO cells are relatively more resistant to PLX4720 compared to LS411N cells. Therefore, to assess the potential involvement of MUC1-C in acquired BRAFi resistance, we established LS411N-BR cells selected for growth in the presence of PLX4720. Of interest and like RKO cells, LS411N-BR cells exhibited upregulation of CDK6, p-RB, cyclin A2 and cyclin B1. In addition, LS411N-BR cells were dependent on MUC1-C for (i) expression of CDK6, p-RB, cyclin A2 and cyclin B1 and (ii) proliferation. These findings suggested that MUC1-C promotes BRAFi resistance, at least in part, by driving cell cycle progression (Fig. 8C). Along these lines, we found that targeting MUC1-C genetically and pharmacologically with the GO-203 inhibitor sensitizes RKO and LS411N-BR cells to PLX4720-mediated inhibition of proliferation as determined by the capacity for colony formation. Unresponsiveness of BRAF(V600E) CRC cells to BRAF inhibition has been linked to reactivation of RTK→RAS→MAPK signaling (6–8, 49). SHP2 functions as an activator of RTK signaling and confers resistance to targeted agents (50–52). Nonetheless, it was not known if SHP2 confers BRAFi resistance in BRAF(V600E) CRCs. Based on the identification of a consensus motif in the MUC1-C cytoplasmic domain for binding of the SHP2 N-terminal SH2 domain, we found that MUC1-C forms a complex

with SHP2. The functional importance of this interaction was documented by the finding that silencing MUC1-C suppresses p-SHP2(Y542) phosphorylation. In addition, targeting MUC1-C with the GO-203 inhibitor disrupted the MUC1-C/SHP2 complex and inhibited p-SHP2(Y542) activation. By contrast, silencing MYC had no effect on SHP2 activation, indicating that MUC1-C activates SHP2 by a MYC-independent mechanism (Fig. 8C). In addition, targeting SHP2 had no apparent effect on the MUC1-C→MYC pathway, which is necessary for NOTCH1 expression and self-renewal capacity (Fig. 8C). These findings supported a model in which MUC1-C integrates MYC and SHP2 signaling in the BRAF(V600E) setting (Fig. 8C).

The CSC state and lineage plasticity confer resistance to targeted anti-cancer agents (41–44, 53, 54). MUC1-C contributes to lineage plasticity by inducing EMT and epigenetic reprogramming with activation of PRC1 and PRC2 (16). In addition, MUC1-C→E2F1 signaling drives the CSC state by activating the SWI/SNF esBAF chromatin remodeling complex and thereby increasing chromatin accessibility and expression of *NOTCH1* and other stemness genes (Fig. 8C) (14, 21, 23). These and other findings have collectively supported dependency of CSCs on MUC1-C for self-renewal, tumorigenicity and the memory response for drug resistance (13–15, 55–58). The present work extends these findings to BRAF(V600E) CRC and supports targeting of MUC1-C for the treatment of patients with these recalcitrant tumors. Importantly, we found that targeting MUC1-C genetically and pharmacologically blocks BRAFi-induced feedback activation of ERK, which confers resistance of BRAF(V600E) CRCs to BRAF inhibition. We also found that targeting MUC1-C blocks BRAFi-induced AKT activation, which has similarly been linked to BRAFi resistance (11). Of note, our results in these class 1 BRAF(V600E) mutant CRC cells may extend to other subgroups, such as those in class 2 with BRAF mutations in codons 597/601 and in class 3 harboring BRAF mutations in codons 594/596 (59). Additional studies will therefore be needed to investigate the involvement of MUC1-C in these less common CRCs with non-BRAF(V600E) mutations, which are reliant on RTKs for MAPK activation (60).

Of potential relevance for the findings in BRAFi resistant CRCs, MUC1-C also confers resistance of CRC, breast cancer and other types of cancer cells to genotoxic anti-cancer agents (55, 61). Targeting MUC1-C reverses that resistance and is synergistic with these agents against DNA damage resistant cancer cells (13, 55, 61). MUC1-C also promotes resistance to targeted agents, such as tamoxifen, trastuzumab and afatinib, and inhibiting MUC1-C function is synergistic with these agents in settings of their corresponding resistant cells (56, 57, 62). These findings and those in the present work indicate that MUC1-C drives pleotropic mechanisms of resistance, which relate to stress-induced memory responses with imprinting of epigenetic reprogramming and chromatin remodeling (13, 14). In this regard, the MUC1-C cytoplasmic domain interacts with effectors, such as STAT3 and NF-kB, which are activated in anti-cancer agent resistant cells and form auto-inductive loops that in turn induce MUC1 expression (14). The present results lend further support to this auto-inductive MUC1-C-driven memory response of BRAF(V600E) CRC cells in association with upregulation of MUC1 expression BRAF(V600E) CRC tumors. Our findings that targeting MUC1-C genetically and pharmacologically with GO-203 reverses BRAFi resistance *in vitro* and in the tumor xenograft studies uncover the potential

importance of anti-MUC1-C agents for the treatment of BRAF(V600E) CRCs. Along these lines, the *in vivo* treatment studies were performed with GO-203 because of the translational importance associated with using this agent rather than DOX-induced MUC1-C silencing. Among potential anti-MUC1-C agents, allogeneic CAR T cells targeting MUC1-C-expressing cancers are now under clinical evaluation (NCT05239143). In addition, an anti-MUC1-C antibody drug conjugate (ADC) is under development with the NCI NExT Program for IND-enabling studies and early phase clinical trials (63). Phase I clinical evaluation of daily intravenous GO-203 administration demonstrated that this agent has an acceptable safety profile for combination studies (13). GO-203 has thus been formulated in nanoparticles for more convenient dosing schedules of once or twice a week in the clinic (45). Taken together with the present findings and the upregulation of MUC1 expression in BRAF(V600E) tumors, the availability of these anti-MUC1-C agents could improve the treatment of patients with this recalcitrant cancer when used alone and in combination with BRAF inhibitors.

Supplementary Material

Refer to Web version on PubMed Central for supplementary material.

Acknowledgements

Research reported in this publication was supported by the National Cancer Institute of the National Institutes of Health under grant numbers CA97098 and CA233084 awarded to DK.

References

1. Clarke CN and Kopetz ES, BRAF mutant colorectal cancer as a distinct subset of colorectal cancer: clinical characteristics, clinical behavior, and response to targeted therapies. J Gastrointest Oncol, 2015. 6:660–667, doi: 10.3978/j.issn.2078-6891.2015.077. [PubMed: 26697199]
2. Di Nicolantonio F, Vitiello PP, Marsoni S, Siena S, Tabernero J, Trusolino L, Bernards R, and Bardelli A, Precision oncology in metastatic colorectal cancer - from biology to medicine. Nat Rev Clin Oncol, 2021. 18:506–525, doi: 10.1038/s41571-021-00495-z. [PubMed: 33864051]
3. Grassi E, Corbelli J, Papiani G, Barbera MA, Gazzaneo F, and Tamberi S, Current therapeutic strategies in BRAF-mutant metastatic colorectal cancer. Front Oncol, 2021. 11:601722, doi: 10.3389/fonc.2021.601722. [PubMed: 34249672]
4. Jang MH, Kim S, Hwang DY, Kim WY, Lim SD, Kim WS, Hwang TS, and Han HS, BRAF-mutated colorectal cancer exhibits distinct clinicopathological features from wild-type BRAF-expressing cancer independent of the microsatellite instability status. J Korean Med Sci, 2017. 32:38–46, doi: 10.3346/jkms.2017.32.1.38. [PubMed: 27914130]
5. Ogino S, Brahmandam M, Kawasaki T, Kirkner GJ, Loda M, and Fuchs CS, Epigenetic profiling of synchronous colorectal neoplasias by quantitative DNA methylation analysis. Mod Pathol, 2006. 19:1083–1090, doi: 10.1038/modpathol.3800618. [PubMed: 16699497]
6. Prahallad A, Sun C, Huang S, Di Nicolantonio F, Salazar R, Zecchin D, Beijersbergen RL, Bardelli A, and Bernards R, Unresponsiveness of colon cancer to BRAF(V600E) inhibition through feedback activation of EGFR. Nature, 2012. 483:100–103, doi: 10.1038/nature10868.
7. Corcoran RB, Ebi H, Turke AB, Coffee EM, Nishino M, Cogdill AP, Brown RD, Della Pelle P, Dias-Santagata D, Hung KE, Flaherty KT, Piris A, Wargo JA, Settleman J, Mino-Kenudson M, and Engelman JA, EGFR-mediated re-activation of MAPK signaling contributes to insensitivity of BRAF mutant colorectal cancers to RAF inhibition with vemurafenib. Cancer Discov, 2012. 2:227–235, doi: 10.1158/2159-8290.CD-11-0341. [PubMed: 22448344]

8. Herr R, Halbach S, Heizmann M, Busch H, Boerries M, and Brummer T, BRAF inhibition upregulates a variety of receptor tyrosine kinases and their downstream effector Gab2 in colorectal cancer cell lines. Oncogene, 2018. 37:1576–1593, doi: 10.1038/s41388-017-0063-5.
9. Corcoran RB, Dias-Santagata D, Bergethon K, Iafrate AJ, Settleman J, and Engelman JA, BRAF gene amplification can promote acquired resistance to MEK inhibitors in cancer cells harboring the BRAF V600E mutation. Sci Signal, 2010. 3:ra84, doi: 10.1126/scisignal.2001148. [PubMed: 21098728]
10. Corcoran RB, Atreya CE, Falchook GS, Kwak EL, Ryan DP, Bendell JC, Hamid O, Messersmith WA, Daud A, Kurzrock R, Pierobon M, Sun P, Cunningham E, Little S, Orford K, Motwani M, Bai Y, Patel K, Venook AP, and Kopetz S, Combined BRAF and MEK inhibition with Dabrafenib and Trametinib in BRAF V600-mutant colorectal cancer. J Clin Oncol, 2015. 33:4023–4031, doi: 10.1200/JCO.2015.63.2471. [PubMed: 26392102]
11. Mao M, Tian F, Mariadason JM, Tsao CC, Lemos R Jr., Dayyani F, Gopal YN, Jiang ZQ, Wistuba II, Tang XM, Bornman WG, Bollag G, Mills GB, Powis G, Desai J, Gallick GE, Davies MA, and Kopetz S, Resistance to BRAF inhibition in BRAF-mutant colon cancer can be overcome with PI3K inhibition or demethylating agents. Clin Cancer Res, 2013. 19:657–667, doi: 10.1158/1078-0432.CCR-11-1446. [PubMed: 23251002]
12. Kufe D, Mucins in cancer: function, prognosis and therapy. Nature Reviews Cancer, 2009. 9:874–885, doi: 10.1038/nrc2761. [PubMed: 19935676]
13. Kufe D, MUC1-C in chronic inflammation and carcinogenesis; emergence as a target for cancer treatment. Carcinogenesis, 2020. 41:1173–1183, doi: 10.1093/carcin/bgaa082. [PubMed: 32710608]
14. Kufe D, Emergence of MUC1 in mammals for adaptation of barrier epithelia Cancers (Basel), 2022. 14:4805, doi: 10.3390/cancers14194805. [PubMed: 36230728]
15. Kufe D, Chronic activation of MUC1-C in wound repair promotes progression to cancer stem cells. J Cancer Metastasis Treat, 2022. 8:Epub 2022 Mar 2031, doi: 10.20517/2394-4722.2022.03.
16. Rajabi H, Hiraki M, and Kufe D, MUC1-C activates polycomb repressive complexes and downregulates tumor suppressor genes in human cancer cells. Oncogene, 2018. 37:2079–2088, doi: 10.1038/s41388-017-0096-9. [PubMed: 29379165]
17. Deng W, Jacobson EC, Collier AJ, and Plath K, The transcription factor code in iPSC reprogramming. Curr Opin Genet Dev, 2021. 70:89–96, doi: 10.1016/j.gde.2021.06.003. [PubMed: 34246082]
18. Singhal N, Graumann J, Wu G, Arauzo-Bravo MJ, Han DW, Greber B, Gentile L, Mann M, and Scholer HR, Chromatin-remodeling components of the BAF complex facilitate reprogramming. Cell, 2010. 141:943–955, doi: 10.1016/j.cell.2010.04.037.
19. Chronis C, Fiziev P, Papp B, Butz S, Bonora G, Sabri S, Ernst J, and Plath K, Cooperative binding of transcription factors orchestrates reprogramming. Cell, 2017. 168:442–459 e420, doi: 10.1016/j.cell.2016.12.016.
20. Chen K, Long Q, Xing G, Wang T, Wu Y, Li L, Qi J, Zhou Y, Ma B, Scholer HR, Nie J, Pei D, and Liu X, Heterochromatin loosening by the Oct4 linker region facilitates Klf4 binding and iPSC reprogramming. EMBO J, 2020. 39:e99165, doi: 10.15252/embj.201899165. [PubMed: 31571238]
21. Hagiwara M, Yasumizu Y, Yamashita N, Rajabi H, Fushimi A, Long MD, Li W, Bhattacharya A, Ahmad R, Oya M, Liu S, and Kufe D, MUC1-C activates the BAF (mSWI/SNF) complex in prostate cancer stem cells. Cancer Res, 2021. 81:1111–1122, doi: 10.1158/0008-5472.CAN-20-2588. [PubMed: 33323379]
22. Hagiwara M, Fushimi A, Yamashita N, Battacharya A, Rajabi H, Long M, Yasumizu Y, Oya M, Liu S, and Kufe D, MUC1-C activates the PBAF chromatin remodeling complex in integrating redox balance with progression of human prostate cancer stem cells. Oncogene, 2021. 40:4930–4940, doi: 10.1038/s41388-021-01899-y. [PubMed: 34163028]
23. Bhattacharya A, Fushimi A, Yamashita N, Hagiwara M, Morimoto Y, Rajabi H, Long MD, Abdulla M, Ahmad R, Street K, Liu S, Liu T, and Kufe D, MUC1-C dictates JUN and BAF-mediated chromatin remodeling at enhancer signatures in cancer stem cells. Mol Cancer Res 2022. 20:556–567, doi: 10.1158/1541-7786.MCR-21-0672. [PubMed: 35022313]

24. Li W, Zhang N, Jin C, Long MD, Rajabi H, Yasumizu Y, Fushimi A, Yamashita N, Hagiwara M, Zheng R, Wang J, Kui L, Singh H, Kharbanda S, Hu Q, Liu S, and Kufe D, MUC1-C drives stemness in progression of colitis to colorectal cancer. JCI Insight, 2020. 5:137112, doi: 10.1172/jci.insight.137112. [PubMed: 32427590]
25. Li C, Zuo D, Liu T, Yin L, Li C, and Wang L, Prognostic and clinicopathological significance of MUC family members in colorectal cancer: a systematic review and meta-analysis. Gastroenterol Res Pract, 2019. 2019:2391670, doi: 10.1155/2019/2391670. [PubMed: 31933627]
26. Biemer-Huttmann AE, Walsh MD, McGuckin MA, Simms LA, Young J, Leggett BA, and Jass JR, Mucin core protein expression in colorectal cancers with high levels of microsatellite instability indicates a novel pathway of morphogenesis. Clin Cancer Res, 2000. 6:1909–1916. [PubMed: 10815915]
27. Fushimi A, Morimoto Y, Ishikawa S, Yamashita N, Bhattacharya A, Daimon T, Rajabi H, Jin C, Hagiwara M, Yasumizu Y, Luan Z, Suo W, Wong K, Withers H, Liu S, Long M, and Kufe D, Dependence on the MUC1-C oncoprotein in classic, variant and non-neuroendocrine small cell lung cancer. Mol Cancer Res, 2022. 20:1379–1390, doi: 10.1158/1541-7786.MCR-22-0165. [PubMed: 35612556]
28. Yamashita N, Fushimi A, Morimoto Y, Bhattacharya A, Hagiwara M, Yamamoto M, Hata T, Shapiro G, Long M, Liu S, and Kufe D, Targeting MUC1-C suppresses chronic activation of cytosolic nucleotide receptors and STING in triple-negative breast cancer. Cancers (Basel), 2022. 14:2580, doi: 10.3390/cancers14112580. [PubMed: 35681561]
29. Yasumizu Y, Rajabi H, Jin C, Hata T, Pitroda S, Long MD, Hagiwara M, Li W, Hu Q, Liu S, Yamashita N, Fushimi A, Kui L, Samur M, Yamamoto M, Zhang Y, Zhang N, Hong D, Takahiro Maeda, Kosaka T, Wong K, Oya M, and Kufe D, MUC1-C regulates lineage plasticity driving progression to neuroendocrine prostate cancer. Nat Commun, 2020. 11:338, doi: 10.1038/s41467-019-14219-6. [PubMed: 31953400]
30. Charan J and Kantharia ND, How to calculate sample size in animal studies? J Pharmacol Pharmacother, 2013. 4:303–306, doi: 10.4103/0976-500X.119726. [PubMed: 24250214]
31. Yang H, Higgins B, Kolinsky K, Packman K, Bradley WD, Lee RJ, Schostack K, Simcox ME, Kopetz S, Heimbrook D, Lestini B, Bollag G, and Su F, Antitumor activity of BRAF inhibitor vemurafenib in preclinical models of BRAF-mutant colorectal cancer. Cancer Res, 2012. 72:779–789, doi: 10.1158/0008-5472.CAN-11-2941. [PubMed: 22180495]
32. Carroll MJ, Parent CR, Page D, and Kreeger PK, Tumor cell sensitivity to vemurafenib can be predicted from protein expression in a BRAF-V600E basket trial setting. BMC Cancer, 2019. 19:1025, doi: 10.1186/s12885-019-6175-2. [PubMed: 31672130]
33. Goel S, Bergholz JS, and Zhao JJ, Targeting CDK4 and CDK6 in cancer. Nat Rev Cancer, 2022. 22:356–372, doi: 10.1038/s41568-022-00456-3. [PubMed: 35304604]
34. Enserink JM and Kolodner RD, An overview of Cdk1-controlled targets and processes. Cell Div, 2010. 5:Article 11 doi: 10.1186/1747-1028-5-11.
35. Enserink JM and Chymkowitch P, Cell cycle-dependent transcription: the cyclin dependent kinase CDK1 is a direct regulator of basal transcription machineries. Int J Mol Sci, 2022. 23, doi: 10.3390/ijms23031293.
36. Hata T, Rajabi H, Takahashi H, Yasumizu Y, Li W, Jin C, Long M, Hu Q, Liu S, Fushimi A, Yamashita N, Kui L, Hong D, Yamamoto M, Miyo M, Hiraki M, Maeda T, Suzuki Y, Samur M, and Kufe D, MUC1-C activates the NuRD complex to drive dedifferentiation of triple-negative breast cancer cells. Cancer Res, 2019. 79:5711–5722, doi: 10.1158/0008-5472.CAN-19-1034. [PubMed: 31519689]
37. Okazaki T, Maeda A, Nishimura H, Kurosaki T, and Honjo T, PD-1 immunoreceptor inhibits B cell receptor-mediated signaling by recruiting src homology 2-domain-containing tyrosine phosphatase 2 to phosphotyrosine. Proc Natl Acad Sci U S A, 2001. 98:13866–13871, doi: 10.1073/pnas.231486598. [PubMed: 11698646]
38. Anselmi M, Calligari P, Hub JS, Tartaglia M, Bocchinfuso G, and Stella L, Structural determinants of phosphopeptide binding to the N-terminal Src homology 2 domain of the SHP2 phosphatase. J Chem Inf Model, 2020. 60:3157–3171, doi: 10.1021/acs.jcim.0c00307. [PubMed: 32395997]

39. Marasco M, Kirkpatrick J, Nanna V, Sikorska J, and Carlomagno T, Phosphotyrosine couples peptide binding and SHP2 activation via a dynamic allosteric network. Comput Struct Biotechnol J, 2021. 19:2398–2415, doi: 10.1016/j.csbj.2021.04.040. [PubMed: 34025932]
40. Ben-Porath I, Thomson MW, Carey VJ, Ge R, Bell GW, Regev A, and Weinberg RA, An embryonic stem cell-like gene expression signature in poorly differentiated aggressive human tumors. Nat Genet, 2008. 40:499–507, doi: 10.1038/ng.127. [PubMed: 18443585]
41. De Angelis ML, Francescangeli F, La Torre F, and Zeuner A, Stem cell plasticity and dormancy in the development of cancer therapy resistance. Front Oncol, 2019. 9:626, doi: 10.3389/fonc.2019.00626. [PubMed: 31355143]
42. Miranda A, Hamilton PT, Zhang AW, Pattnaik S, Becht E, Mezheyeuski A, Bruun J, Micke P, de Reynies A, and Nelson BH, Cancer stemness, intratumoral heterogeneity, and immune response across cancers. Proc Natl Acad Sci USA, 2019. 116:9020–9029, doi: 10.1073/pnas.1818210116. [PubMed: 30996127]
43. Malta TM, Sokolov A, Gentles AJ, Burzykowski T, Poisson L, Weinstein JN, Kaminska B, Huelsken J, Omberg L, Gevaert O, Colaprico A, Czerwinska P, Mazurek S, Mishra L, Heyn H, Krasnitz A, Godwin AK, Lazar AJ, Cancer Genome Atlas Research N, Stuart JM, Hoadley KA, Laird PW, Noushmehr H, and Wiznerowicz M, Machine learning identifies stemness features associated with oncogenic dedifferentiation. Cell, 2018. 173:338–354 e315, doi: 10.1016/j.cell.2018.03.034.
44. Quintanal-Villalonga A, Chan JM, Yu HA, Pe'er D, Sawyers CL, Sen T, and Rudin CM, Lineage plasticity in cancer: a shared pathway of therapeutic resistance. Nat Rev Clin Oncol, 2020. 17:360–371, doi: 10.1038/s41571-020-0340-z. [PubMed: 32152485]
45. Hasegawa M, Sinha RK, Kumar M, Alam M, Yin L, Raina D, Kharbanda A, Panchamoorthy G, Gupta D, Singh H, Kharbanda S, and Kufe D, Intracellular targeting of the oncogenic MUC1-C protein with a novel GO-203 nanoparticle formulation. Clin Cancer Res, 2015. 21:2338–23347, doi: 10.1158/1078-0432.CCR-14-3000. [PubMed: 25712682]
46. Yamashita N, Morimoto Y, Fushimi A, Ahmad R, Bhattacharya A, Daimon T, Haratake N, Inoue Y, Ishikawa S, Yamamoto M, Hata T, Akiyoshi S, Hu Q, Liu T, Withers H, Liu S, Shapiro G, Yoshizumi T, Long M, and Kufe D, MUC1-C dictates PBRM1-mediated chronic induction of interferon signaling, DNA damage resistance and immunosuppression in triple-negative breast cancer. Mol Canc Res, 2022:Epub: Nov 29, doi: 10.1158/1541-7786.MCR-22-0772.
47. Bouillez A, Rajabi H, Pitroda S, Jin C, Alam M, Kharbanda A, Tagde A, Wong K, and Kufe D, Inhibition of MUC1-C suppresses MYC expression and attenuates malignant growth in KRAS mutant lung adenocarcinomas. Cancer Res, 2016. 76:1538–1548, doi: 10.1158/0008-5472.CAN-15-1804. [PubMed: 26833129]
48. Dang CV MYC on the path to cancer. Cell, 2012. 149:22–35, doi: 10.1016/j.cell.2012.03.003. [PubMed: 22464321]
49. Herr R, Kohler M, Andrlova H, Weinberg F, Moller Y, Halbach S, Lutz L, Mastroianni J, Klose M, Bittermann N, Kowar S, Zeiser R, Olayioye MA, Lassmann S, Busch H, Boerries M, and Brummer T, B-Raf inhibitors induce epithelial differentiation in BRAF-mutant colorectal cancer cells. Cancer Res, 2015. 75:216–229, doi: 10.1158/0008-5472.CAN-13-3686.
50. Liu X, Zheng H, Li X, Wang S, Meyerson HJ, Yang W, Neel BG, and Qu CK, Gain-of-function mutations of Ptpn11 (Shp2) cause aberrant mitosis and increase susceptibility to DNA damage-induced malignancies. Proc Natl Acad Sci U S A, 2016. 113:984–989, doi: 10.1073/pnas.1508535113. [PubMed: 26755576]
51. Prahallad A, Heynen GJ, Germano G, Willems SM, Evers B, Vecchione L, Gambino V, Lieftink C, Beijersbergen RL, Di Nicolantonio F, Bardelli A, and Bernards R, PTPN11 Is a central node in intrinsic and acquired cresistance to targeted cancer drugs. Cell Rep, 2015. 12:1978–1985, doi: 10.1016/j.celrep.2015.08.037. [PubMed: 26365186]
52. Asmamaw MD, Shi XJ, Zhang LR, and Liu HM, A comprehensive review of SHP2 and its role in cancer. Cell Oncol (Dordr), 2022. 45:729–753, doi: 10.1007/s13402-022-00698-1. [PubMed: 36066752]
53. Sharma SV, Lee DY, Li B, Quinlan MP, Takahashi F, Maheswaran S, McDermott U, Azizian N, Zou L, Fischbach MA, Wong KK, Brandstetter K, Wittner B, Ramaswamy S, Classon M, and

Settleman J, A chromatin-mediated reversible drug-tolerant state in cancer cell subpopulations. Cell, 2010. 141:69–80, doi: 10.1016/j.cell.2010.02.027. [PubMed: 20371346]

54. Flavahan WA, Gaskell E, and Bernstein BE, Epigenetic plasticity and the hallmarks of cancer. Science, 2017. 357:eaal2380, doi: 10.1126/science.aal2380. [PubMed: 28729483]
55. Uchida Y, Raina D, Kharbanda S, and Kufe D, Inhibition of the MUC1-C oncoprotein is synergistic with cytotoxic agents in treatment of breast cancer cells. Cancer Biol Ther, 2013. 14:127–134, doi: 10.4161/cbt.22634. [PubMed: 23114713]
56. Kharbanda A, Rajabi H, Jin C, Raina D, and Kufe D, Oncogenic MUC1-C promotes tamoxifen resistance in human breast cancer. Mol Cancer Res, 2013. 11:714–723, doi: 10.1158/1541-7786.MCR-12-0668. [PubMed: 23538857]
57. Kharbanda A, Rajabi H, Jin C, Tchaicha J, Kikuchi E, Wong K, and Kufe D, Targeting the oncogenic MUC1-C protein inhibits mutant EGFR-mediated signaling and survival in non-small cell lung cancer cells. Clin Cancer Res, 2014. 20:5423–5434, doi: 10.1158/1078-0432.CCR-13-3168. [PubMed: 25189483]
58. Shigeta K, Hasegawa M, Kikuchi E, Yasumizu Y, Kosaka T, Mizuno R, Mikami S, Miyajima A, Kufe D, and Oya M, Role of the MUC1-C oncoprotein in the acquisition of cisplatin resistance by urothelial carcinoma. Cancer Sci, 2020. 111:3639–3652, doi: 10.1111/cas.14574. [PubMed: 32677159]
59. Schirripa M, Biason P, Lonardi S, Pella N, Pino MS, Urbano F, Antoniotti C, Cremolini C, Corallo S, Pietrantonio F, Gelsomino F, Cascinu S, Orlandi A, Munari G, Malapelle U, Saggio S, Fontanini G, Rugge M, Mescoli C, Lazzi S, Reggiani Bonetti L, Lanza G, Dei Tos AP, De Maglio G, Martini M, Bergamo F, Zagonel V, Loupakis F, and Fassan M, Class 1, 2, and 3 BRAF-mutated metastatic colorectal cancer: a detailed clinical, pathologic, and molecular characterization. Clin Cancer Res, 2019. 25:3954–3961, doi: 10.1158/1078-0432.CCR-19-0311. [PubMed: 30967421]
60. Kotani H, Adachi Y, Kitai H, Tomida S, Bando H, Faber AC, Yoshino T, Voon DC, Yano S, and Ebi H, Distinct dependencies on receptor tyrosine kinases in the regulation of MAPK signaling between BRAF V600E and non-V600E mutant lung cancers. Oncogene, 2018. 37:1775–1787, doi: 10.1038/s41388-017-0035-9. [PubMed: 29348459]
61. Ren J, Agata N, Chen D, Li Y, Yu W, Huang L, Raina D, Chen W, Kharbanda S, and Kufe D, Human MUC1 carcinoma-associated protein confers resistance to genotoxic anti-cancer agents. Cancer Cell, 2004. 5:163–175, doi: 10.1016/s1535-6108(04)00020-0. [PubMed: 14998492]
62. Raina D, Uchida Y, Kharbanda A, Rajabi H, Panchamoorthy G, Jin C, Kharbanda S, Scaltriti M, Baselga J, and Kufe D, Targeting the MUC1-C oncoprotein downregulates HER2 activation and abrogates trastuzumab resistance in breast cancer cells. Oncogene, 2014. 33:3422–3431, doi: 10.1038/onc.2013.308. [PubMed: 23912457]
63. Panchamoorthy G, Jin C, Raina D, Bharti A, Yamamoto M, Adeebge D, Zhao Q, Bronson R, Jiang S, Li L, Suzuki Y, Tagde A, Ghoroghchian P, Wong K-K, Kharbanda S, and Kufe D, Targeting the human MUC1-C oncoprotein with an antibody-drug conjugate. JCI Insight, 2018. 3:e99880, doi: 10.1172/jci.insight.99880. [PubMed: 29925694]

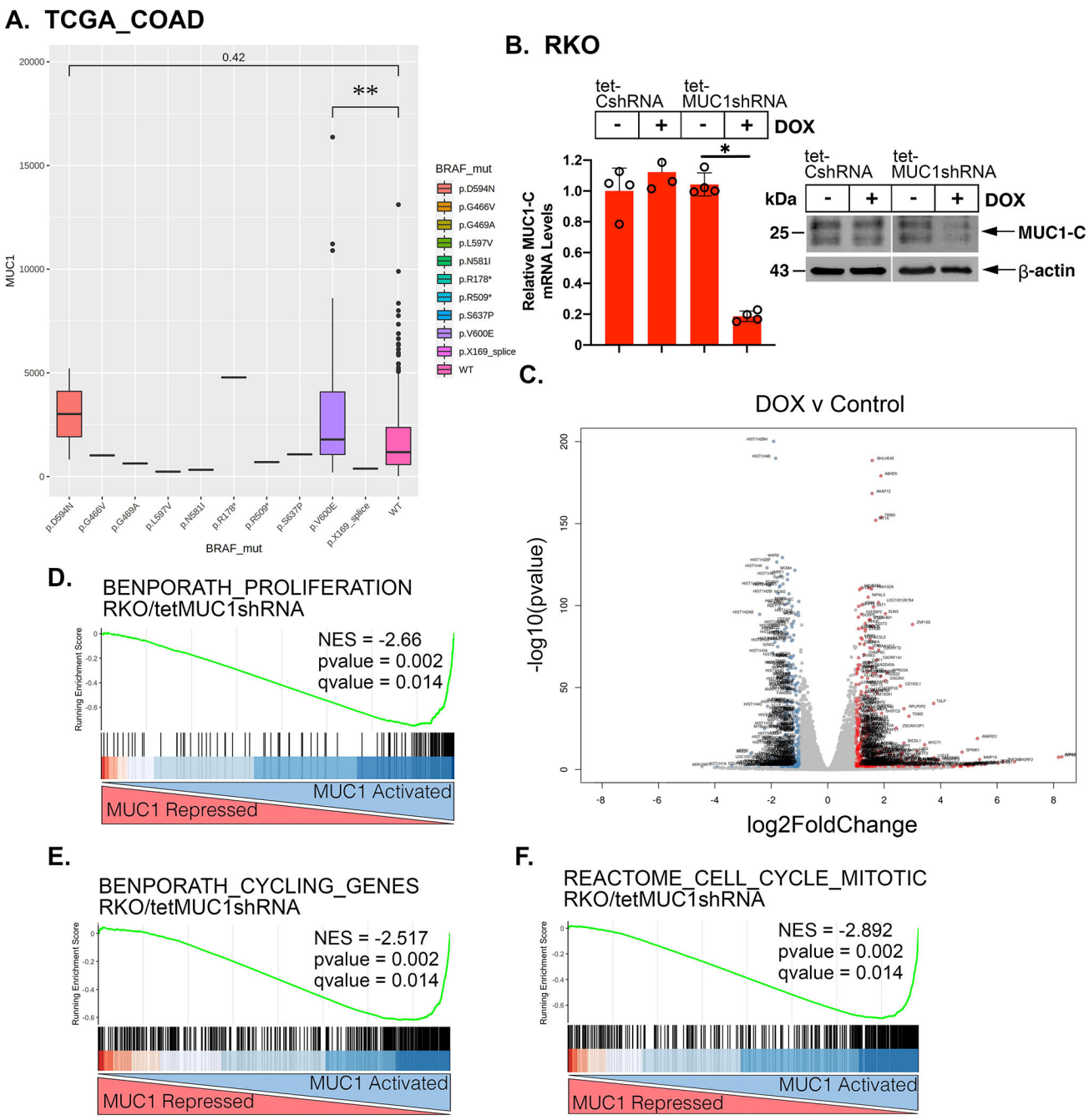

Figure 1. MUC1-C regulates cell cycle genes in RKO BRAF(V600E) cells.

A. Analysis of MUC1 expression in the indicated CRC tumor types using the TCGA-COAD dataset. **B.** RKO/tet-CshRNA and RKO/tet-MUC1shRNA cells treated with vehicle or 500 ng/ml DOX for 7 days were analyzed for MUC1-C mRNA levels by qRT-PCR. The results (mean±SD of four determinations) are expressed as relative levels compared to that obtained for vehicle-treated cells (assigned a value of 1) (left). Lysates were immunoblotted with antibodies against the indicated proteins (right). **C.** RNA-seq was performed in triplicate on RKO/tet-MUC1shRNA cells treated with vehicle or DOX for 7 days. The datasets were analyzed for effects of MUC1-C silencing on down- and upregulated

genes as depicted in the Volcano plot. **D-F.** GSEA of RNA-seq data from control and DOX-treated RKO/tet-MUC1shRNA cells using the BENPORATH_PROLIFERATION (**D**), BENPORATH_CYCLING_GENES (**E**) and REACTOME_CELL CYCLE_MITOTIC (**F**) gene signatures.

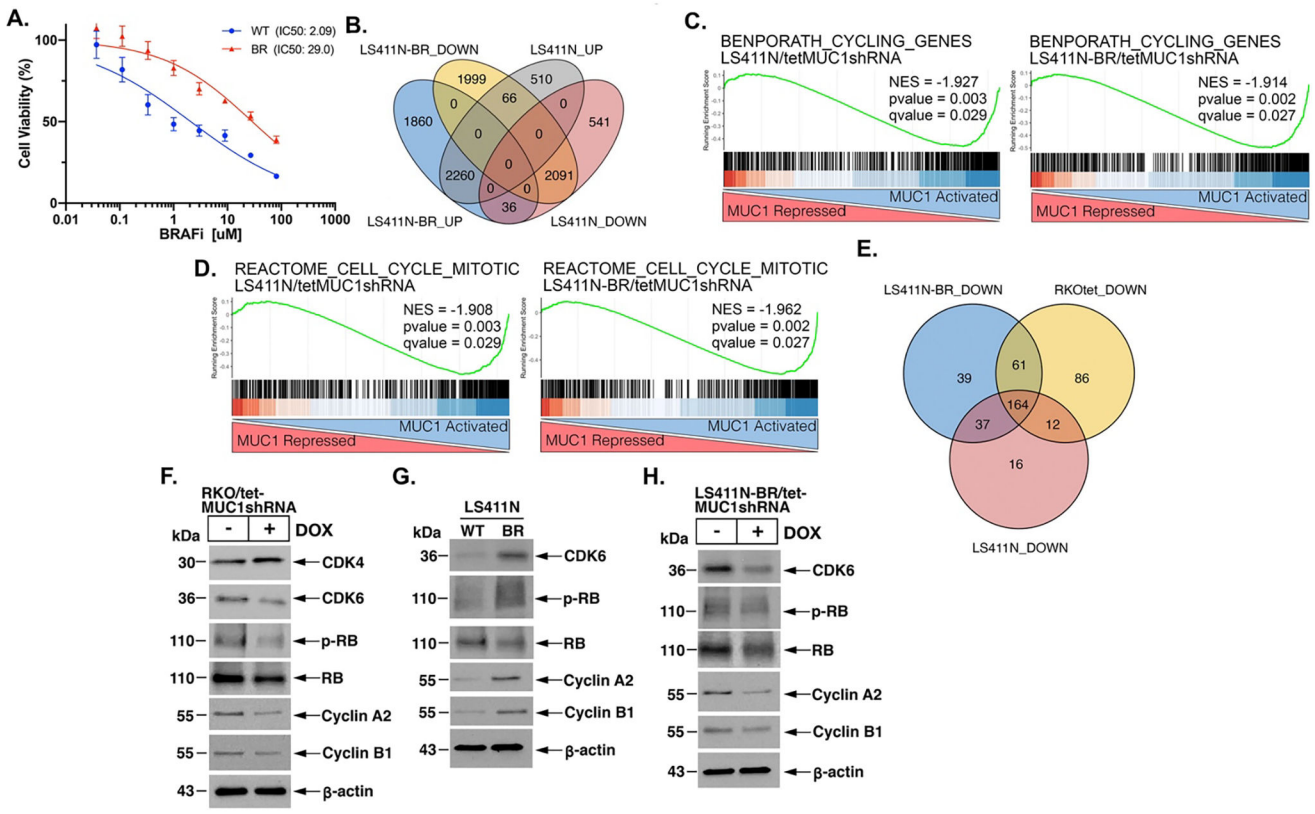

Figure 2. MUC1-C drives cell cycle gene expression in LS411N BRAF(V600E) cells with acquired BRAFi resistance.

A. LS411N BRAF(V600E) cells were selected for growth in increasing concentrations of PLX4720 to establish BRAFi-resistant LS411N-BR cells. LS411N and LS411N-BR cells incubated in the presence of the indicated PLX4720 (PLX) concentrations for 96 hours were analyzed for cell viability by AlamarBlue staining. The results are expressed as the mean±SD of six determinations. Indicated are the calculated IC50 values. **B.** RNA-seq was performed in triplicate on LS411N/tet-MUC1shRNA and LS411N-BR/tet-MUC1shRNA cells treated with vehicle or DOX for 7 days. The datasets were analyzed for effects of MUC1-C silencing on overlapping down- and up-regulated genes. **C and D.** GSEA of RNA-seq data from control and DOX-treated LS411N/tet-MUC1shRNA (left) and LS411N-BR/tet-MUC1shRNA (right) cells using the BENPORATH_CYCLING_GENES (**C**) and REACTOME_CELL CYCLE_MITOTIC (**D**) gene signatures. **E.** Overlap of MUC1-C-activated genes in the indicated cells. **F.** Lysates from RKO/tet-MUC1shRNA cells treated with vehicle or DOX for 7 days were immunoblotted with antibodies against the indicated proteins. **G and H.** Lysates from (i) LS411N and LS411N-BR cells (**G**), and (ii) LS411N-BR/tet-MUC1shRNA cells treated with vehicle or DOX for 7 days (**H**) were immunoblotted with antibodies against the indicated proteins.

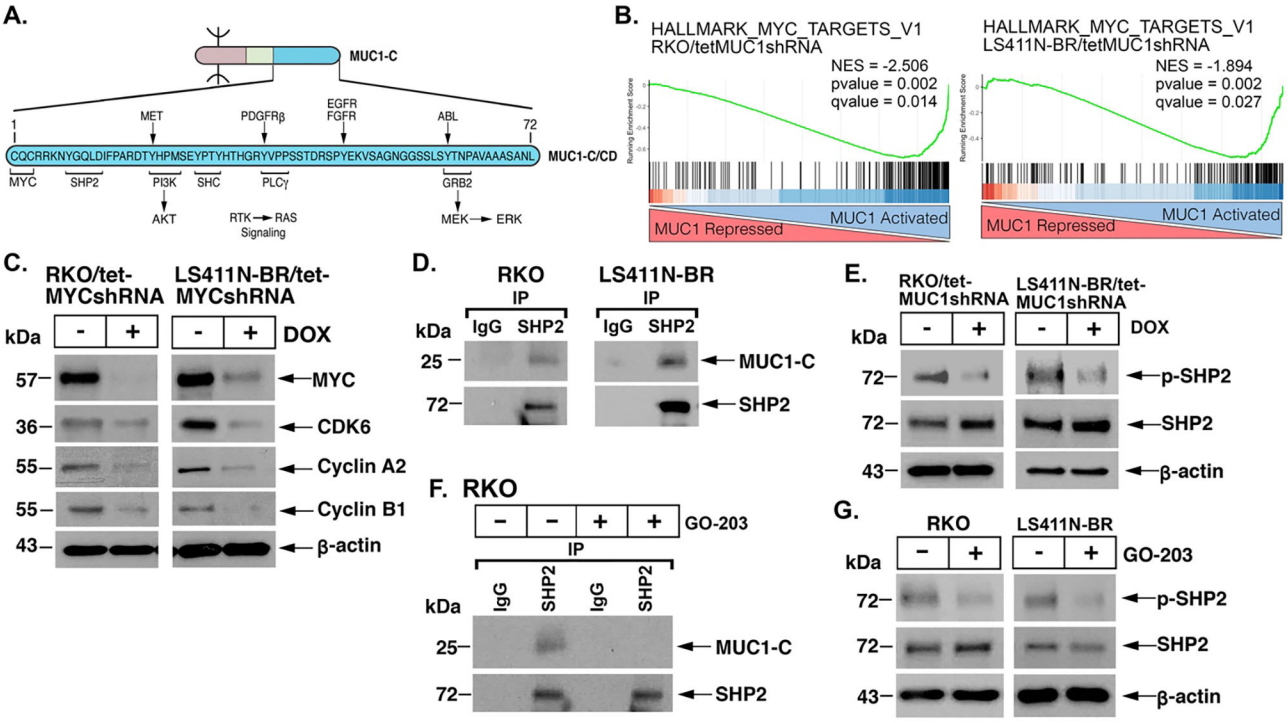

Figure 3. MUC1-C regulates activation of MYC and SHP2 signaling in BRAF(V600E) CRC cells.

A. Schema of the MUC1-C subunit with the 58 aa extracellular domain (pink), 28 aa transmembrane domain (yellow) and 72 aa cytoplasmic domain (CD; blue). The CQC motif binds directly to the MYC HLH LZ domain and regulates MYC target genes. Also depicted are sites phosphorylated by the indicated TKs and the resulting binding motifs for SH2 domains of downstream effectors. **B.** GSEA of RNA-seq data from control and DOX-treated RKO/tet-MUC1shRNA and LS411N-BR/tet-MUC1shRNA cells using the HALLMARK_MYC_TARGETS_V1 gene signature. **C.** Lysates from RKO/tet-MYCshRNA and LS411N-BR/tet-MYCshRNA cells treated with vehicle or DOX for 7 days were immunoblotted with antibodies against the indicated proteins. **D.** Lysates from RKO and LS411N-BR were precipitated with a control IgG or anti-SHP2. The precipitates were immunoblotted with antibodies against the indicated proteins. **E.** Lysates from RKO/tet-MUC1shRNA and LS411N-BR/tet-MUC1shRNA cells treated with vehicle or DOX for 7 days were immunoblotted with antibodies against the indicated proteins. **F.** Lysates from RKO cells left untreated or treated with 5 μM GO-203 for 48 hours were precipitated with a control IgG or anti-SHP2. The precipitates were immunoblotted with antibodies against the indicated proteins. **G.** Lysates from RKO and LS411N-BR cells left untreated or treated with 5 μM GO-203 for 48 hours were immunoblotted with antibodies against the indicated proteins.

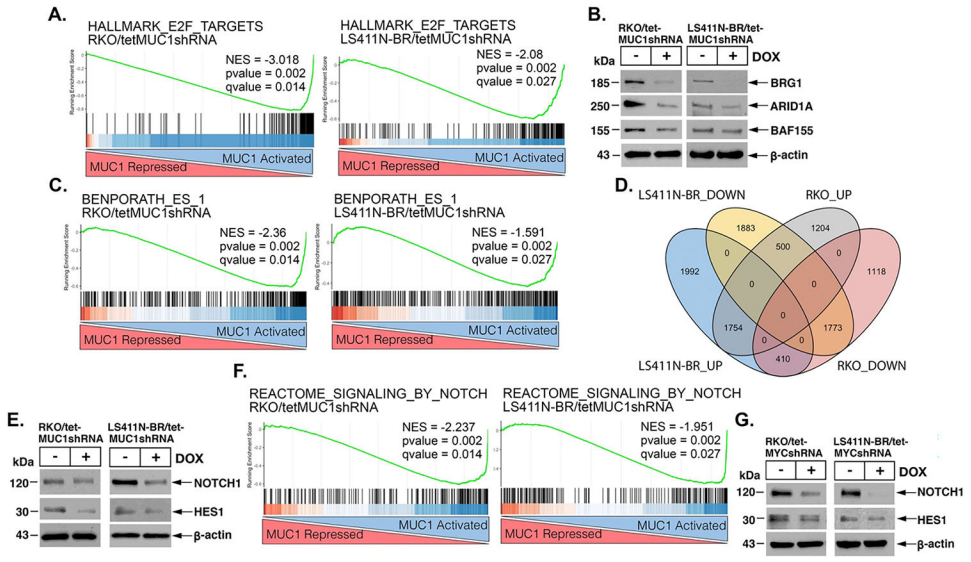

Figure 4. MUC1-C activates esBAF and stemness-associated genes in BRAF(V600E) CRC cells.

A. GSEA of RNA-seq data from control and DOX-treated RKO/tet-MUC1shRNA (left) and LS411N-BR/tet-MUC1shRNA (right) cells using the HALLMARK_E2F_TARGETS gene signature. **B.** Lysates from RKO/tet-MUC1shRNA and LS411N-BR/tet-MUC1shRNA cells treated with vehicle or DOX for 7 days were immunoblotted with antibodies against the indicated proteins. **C.** GSEA of RNA-seq data from control and DOX-treated RKO/tet-MUC1shRNA (left) and LS411N-BR/tet-MUC1shRNA (right) cells using the BENPORATH_ES_1 gene signature. **D.** Overlap of MUC1-C-regulated genes in the indicated cells. **E.** Lysates from RKO/tet-MUC1shRNA and LS411N-BR/tet-MUC1shRNA cells treated with vehicle or DOX for 7 days were immunoblotted with antibodies against the indicated proteins. **F.** GSEA of RNA-seq data from control and DOX-treated RKO/tet-MUC1shRNA (left) and LS411N-BR/tet-MUC1shRNA (right) cells using the REACTOME_SIGNALING_BY_NOTCH gene signature. **G.** Lysates from RKO/tet-MYCshRNA and LS411N-BR/tet-MYCshRNA cells treated with vehicle or DOX for 7 days were immunoblotted with antibodies against the indicated proteins.

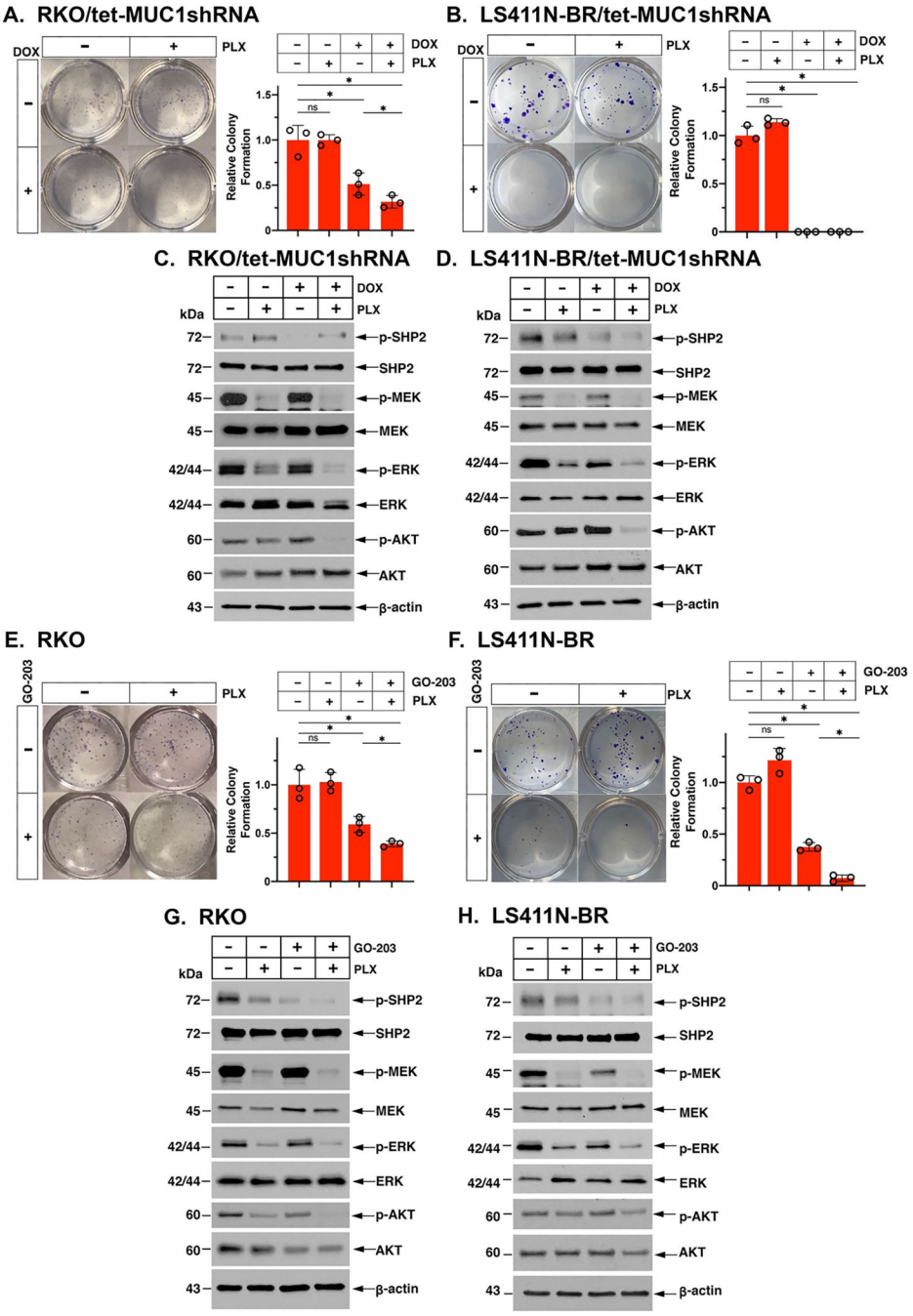

Figure 5. Targeting MUC1-C potentiates the growth inhibitory effects of PLX4720 on BRAFi-resistant BRAF(V600E) CRC cells.

A and B. Representative images of colonies for RKO/tet-MUC1shRNA (**A**) and LS411N-BR (**B**) cells treated with vehicle or DOX for 7 days and then for an additional 7 and 10 days, respectively, in the absence and presence of 2 μM PLX4720. Colony number is expressed as the mean±SD of three independent replicates relative to that obtained for untreated cells. **C and D.** Lysates from RKO cells (**C**) and LS411N-BR cells (**D**). **E-H.** Representative images of colonies for RKO (**E**) and LS411N-BR (**F**) cells treated with

vehicle or 5 μM GO-203 for 7 and 10 days, respectively, in the absence and presence of 2 μM PLX4720. Colony number is expressed as the mean±SD of three independent replicates relative to that obtained for untreated cells. Lysates were immunoblotted with antibodies against the indicated proteins (**G,H**).

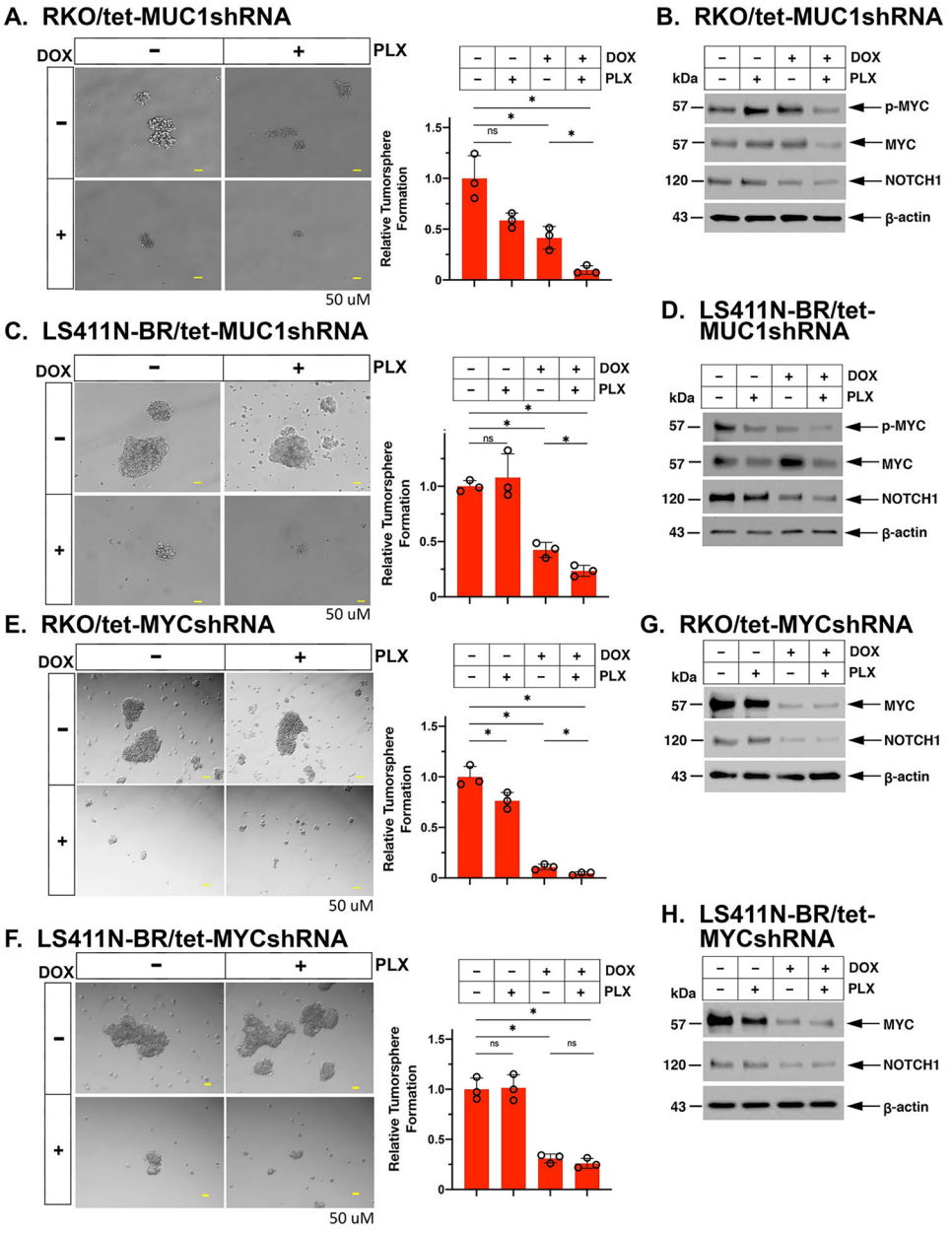

Figure 6. Targeting MUC1-C potentiates the effects of PLX4720 on self-renewal capacity of BRAFi-resistant BRAF(V600E) CRC cells.

A and B. Representative images of tumorspheres for RKO/tet-MUC1shRNA cells treated with vehicle or DOX for 7 days and then for an additional 7 days in the absence and presence of 2 μM PLX4720. Bar represents 50 microns. Tumorsphere formation is expressed as the mean±SD of three independent replicates relative to that obtained for untreated cells (**A**). Lysates were immunoblotted with antibodies against the indicated proteins (**B**). **C and D.** Representative images of tumorspheres for LS411N-BR/tet-MUC1shRNA cells treated with vehicle or DOX for 7 days and then for an additional 7 days in the absence and presence of 2 μM PLX4720. Tumorsphere formation is expressed as the mean±SD of three independent replicates relative to that obtained for untreated cells (**C**). Lysates were

immunoblotted with antibodies against the indicated proteins (**D**). **E and F.** Representative images of tumorspheres for RKO/tet-MYCshRNA (**E**) and LS411N-BR/tet-MYCshRNA (**F**) cells treated with vehicle or DOX for 7 days and then for an additional 7 days in the absence and presence of 2 μM PLX4720. Tumorsphere formation is expressed as the mean±SD of three independent replicates relative to that obtained for untreated cells. **G and H.** Lysates were immunoblotted with antibodies against the indicated proteins.

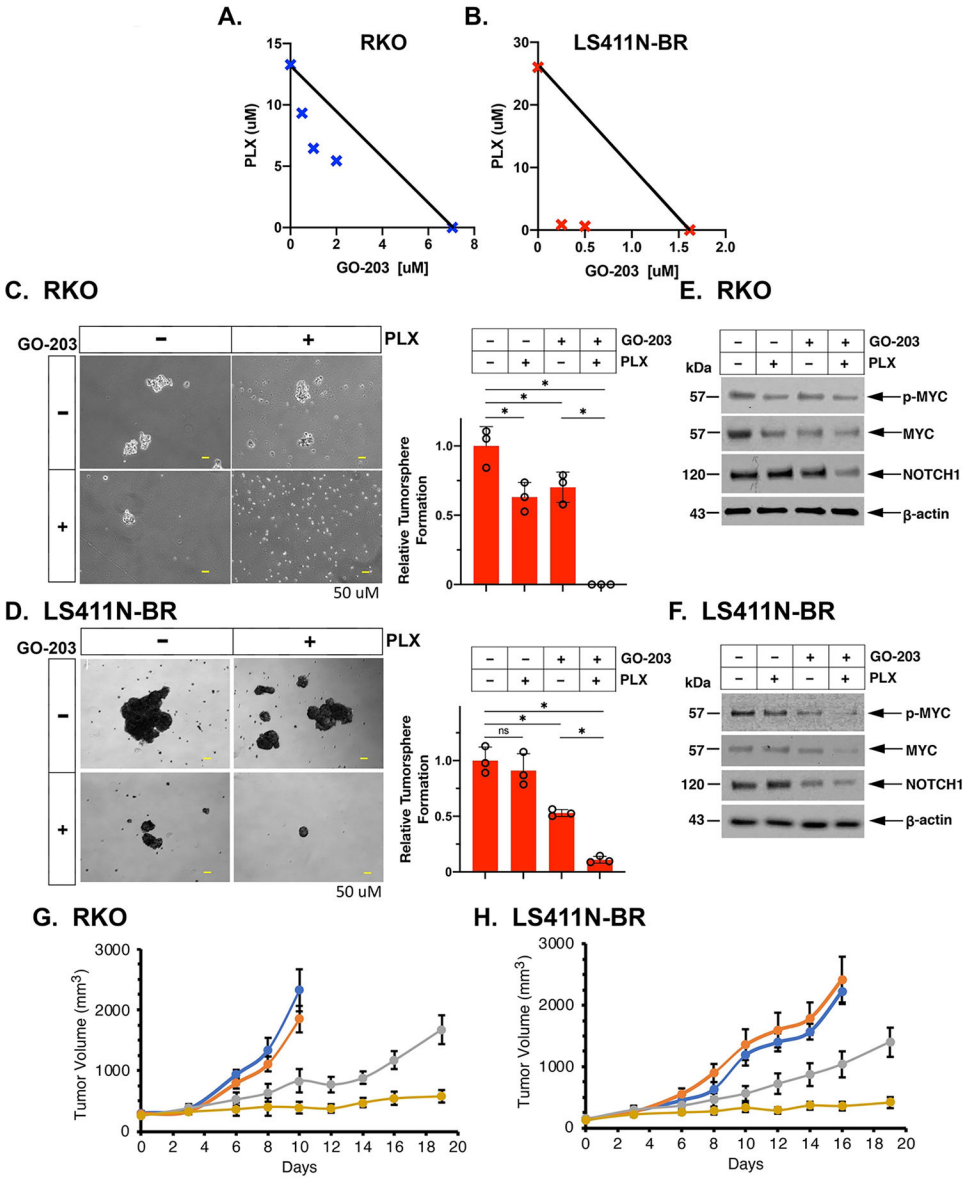

Figure 7. Targeting MUC1-C reverses BRAFi resistance in BRAF(V600E) CRC tumors.

A and B. Cells were left untreated or treated with 0.5, 1 and 2 μM GO-203 **(A)** or 0.25 and 0.5 μM GO-203 **(B)** in the presence of the indicated concentrations of PLX4720. Cell viability was assessed by Alamar blue staining and used to calculate the IC50 values of PLX4720 at each concentration of GO-203. Values under the additive line were denoted as synergistic. **C and D.** Representative images of tumorspheres for RKO (**C**) and LS411N-BR (**D**) cells treated with vehicle or 5 μM GO-203 in the absence and presence of 2 μM PLX4720 for 7 days. Tumorsphere formation is expressed as the mean±SD of three independent replicates relative to that obtained for untreated cells. Lysates were immunoblotted with antibodies against the indicated proteins (**E,F**). **G and H.** Six-week old nude mice were injected subcutaneously in the flank with 1×10^6 RKO (**G**) or 3×10^6 LS411N-BR (**H**) cells. Mice pair-matched into four groups **of 6 mice each** when tumors reached 100–150 mm^3 were treated with vehicle control (blue), PLX4720 (orange),

GO-203 (grey), and GO-203 plus PLX4720 (yellow) for 19 days. Tumor volumes are expressed as the mean±SEM for six mice. These studies were terminated on day 19 when the GO-203-treated mice were sacrificed because of tumors exceeding a volume permitted in the protocol.

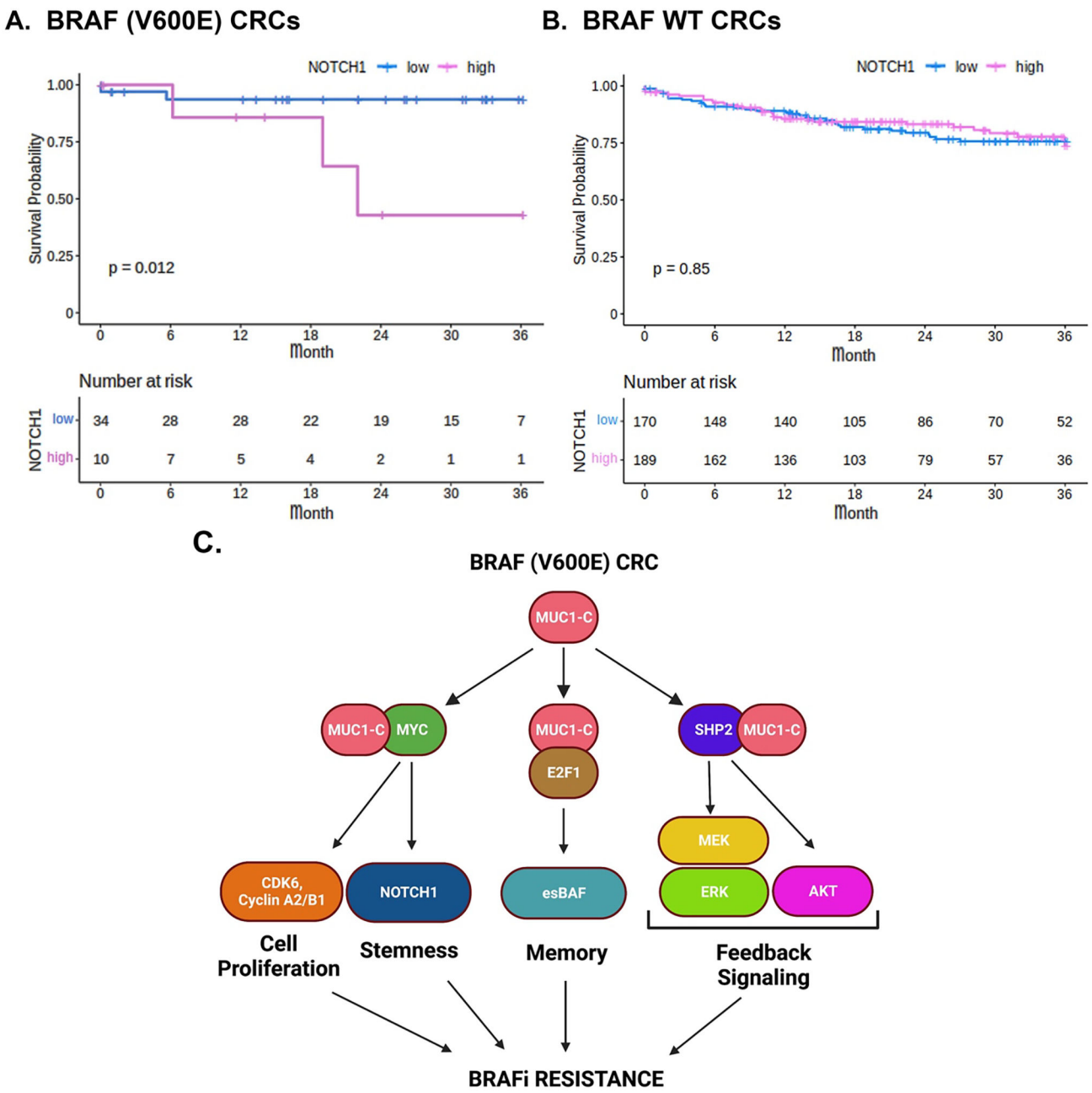

Figure 8. Dependence of BRAF(V600E) CRC cells on MUC1-C for self-renewal and BRAFi resistance.

A and B. Kaplan-Meier (KM) curves for overall survival of patients with BRAF (V600E) (**A**) and BRAF WT (**B**) CRCs. Purple and blue lines show KM curves of patients with NOTCH1-high and NOTCH1-low tumors, respectively. **C.** Proposed model based on the findings that MUC1-C forms complexes with MYC and SHP2 in BRAF(V600E) CRC cells. The MUC1-C®MYC pathway induces effectors of cell cycle progression and the NOTCH1 stemness factor in driving self-renewal and tumorigencity. MUC1-C®E2F1 signaling induces esBAF with increases in chromatin accessibility and activation of genes encoding stemness factors, such as NOTCH1, and the memory response. In

addition, MUC1-C associates with SHP2 and is necessary for p-SHP2(Y542) activation. MUC1-C→p-SHP2(Y542) signaling induces p-MEK, p-ERK and p-AKT, which promote BRAFi resistance by feedback stimulation of RTKs. Targeting MUC1-C genetically and pharmacologically suppresses (i) p-SHP2(Y542) activation, (ii) induction of p-MEK, p-ERK and p-AKT, and (iii) BRAFi resistance. In this way, MUC1-C-induced activation of the MYC, E2F1 and SHP2 pathways integrates the CSC state with targeted BRAF(V600E) inhibitor resistance.